

Coastal Wave Reanalysis in Hue Beach, South China Sea

Tran Thi Khuyen

Graduate Student

Graduate School for International Development and Cooperation
Hiroshima University,
1-5-1 Kagamiyama, Higashi-Hiroshima-shi, Hiroshima 739-8529, Japan

Takao YAMASHITA

Professor

Graduate School for International Development and Cooperation
Hiroshima University,
1-5-1 Kagamiyama, Higashi-Hiroshima-shi, Hiroshima 739-8529, Japan

Abstract

Wave characteristics along the Vietnam coasts facing the South China Sea in which well-organized wave observations have not been developed, were made clear in this study using the ocean wave reanalysis data provided by WW3_NOAA that is global analysis program by the third generation ocean wave model, WW3. Hourly changes in the significant wave height, wave period and wave direction in the offshore waves in the northern, north-central, south-central central, and southern coasts have been analyzed since February, 2005 up to December 2014.

Then, in order to analyze the wave characteristics in the coastal zone, wave deformation computation by shallow water wave model SWAN was carried in 2006 at the north-central Vietnam coast, Hue. As wave boundary conditions in this case, significant wave height, the peak period and peak wave direction of WW3_NOAA were imposed by using the SEGMENT boundary method. In October, 2006, the shallow wave observation data at Hue coast was available to compare the output of SWAN wave analysis as a brief validation of the model. As well as this model validation, the database of shallow water wave fields and the shear stress distribution of breaking waves in the surf zone have been established, as a coastal wave dataset in Hue coastal zone in 2006 which provides the hourly nearshore wave parameters together with white cap dissipation rate and depth-induced breaking shear stresses extending 100 W/m² in the surfzone.

Key words: global ocean wave reanalysis data WW3_NOAA, shallow wave model SWAN, South China Sea.

1. Introduction

Vietnam is lied on the Eastern margin of the Indochinese Peninsula, in tropical monsoon area and has a long coastline covering from north to south approximately 3260 km in length which brings both advantages and difficulties to the country. Besides having a great opportunity to develop a marine economy, Vietnam also faces huge risks such as coastal erosion, flooding, and seawater intrusion that become more serious over years (Tran, T.T. et al, 2013¹⁾). Therefore, protecting the coastline and the coastal community is the first priority of the Vietnamese government's strategy to develop its marine-related economy.

From the above demands, nearshore wave data are very necessary because they play an important role in identifying protective solutions for each type of coasts. However, the hydro-meteorological observations in Vietnam are still very limited. Even though the country has 18 oceanographic stations along its coasts, its network of monitoring station is very poor resulting in a huge dearth of coastal wave data for almost all of the beaches along the Vietnamese territory.

Together with scientific development and widely shared data, United States, National Oceanic and Atmospheric Administration (NOAA) provides offshore-wave data around the world. These data are the direct output of the ocean wave simulation model, WaveWatch III (WW3). Also, they are called reanalysis of offshore wave data because of being created via an unchanging data assimilation scheme and model which ingest all available observations every 6 hours over the period being analyzed.

To obtain coastal wave data, it is possible to use a shallow water wave simulation model, SWAN. This is the most prevailing model and can be used to simulate wave propagation from the offshore to the nearshore with input boundary data of offshore waves, surface wind speeds and seabed topography for the target coastal area. Using numerical models to analyze coastal waves is a useful method because the models can simulate all past and present conditions and predict the changing trend of coastal wave field in the future in whole area of simulation domain.

Thua Thien Hue (also called Hue) province is located in the central region of Vietnam (Figure 1). This coastal province has open-sandy beach with a total coastline of approximately 128 km in length and is characterized as a micro-tidal, wave-dominated coastal environment. Under tropical monsoon climate conditions, Hue faces serious risks such as flooding and erosion that threaten the safety and economic development of coastal communities. There is about 30% of the total coastline in Hue province has been seriously eroded under the impact of storms every year (Tran, T.T. et al, 2013¹). Furthermore, oceanographic observation stations have not yet been established along the coasts of the province. As coastal hazards is getting more serious, it becomes increasingly necessary to understand more details about coastal wave characteristics to protect coastlines more effectively. Meanwhile, Hue province still lacks of coastal wave parameters, such as wave height, wave direction, and wave period, to identify the detailed wave climate in shallow water to design suitable solutions for beach protection and preservation. Given the above issues, this research aim to increase the fundamental understanding of the wave regime in Hue coast by analyzing offshore wave characteristics and coastal wave parameters simulated by SWAN model.

2. Offshore Wave Reanalysis

2.1 Global ocean wave reanalysis, WW3-NOAA

US, NOAA provides global wave reanalysis data that are output results from the model WaveWatch III (WW3) version 2.22, a third generation wave model developed at NOAA/NCEP in the spirit of the WAM model (WAMDIG 1988²). It is a further development of the WaveWatch model developed at the Delft University of Technology (Tolman, 1991³) and of the WaveWatch II model developed at NASA's Goddard Space Flight Center. WW3, however, differs from its predecessors in many important ways, such as the governing equations, the model structure, the numerical methods and the physical parameterizations.

NOAA also supplies spectral partitioning of global wave data which allows the identification of components and the grouping of wave systems from spatially and temporally distributed observations of directional wave spectra. The frequency and direction domains associated with each dominant peak in a wave spectrum form a spectral partition that is associated with that particular wave component as in the Figure 2. In order to use offshore wave data provided by NOAA, the total wave field was employed in this study.

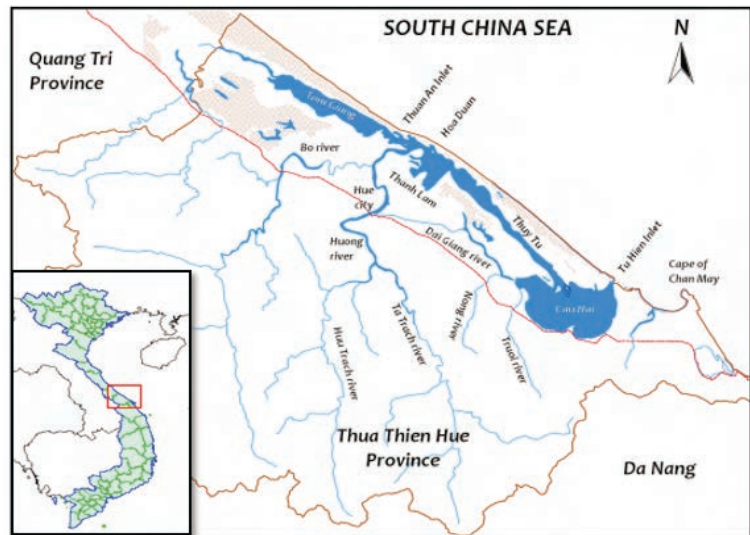


Figure 1. The Hue province in North Central of Vietnam.

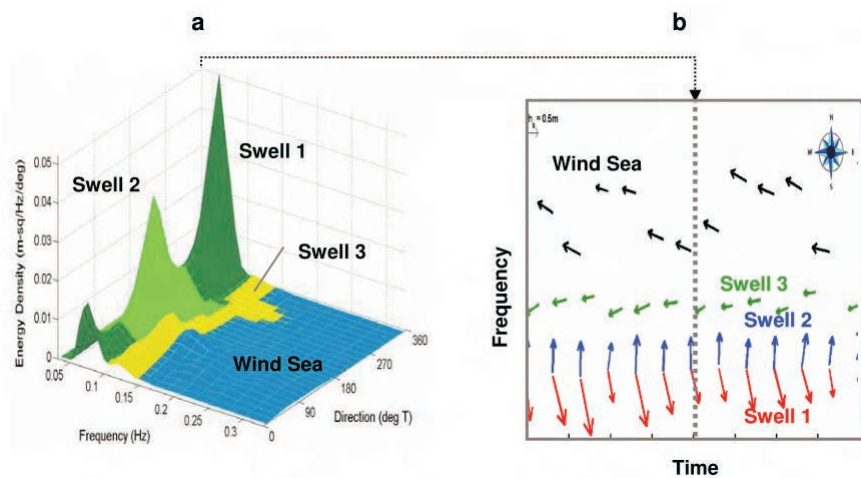


Figure 2. WW3-NOAA wave spectral partition. (a) Spectral components vs (b) Evolution of wave partition height, peak frequency and mean direction of wind waves and swells. (from J. L. Hanson et. al., 2009⁴).

2.2 Validation of offshore wave database of WW3_NOAA

The accuracy of WW3_NOAA reanalysis data should be checked by comparing with observation. Japan's reliable wave observation system NOWPHAS (Nationwide Ocean Wave information network for Ports and HARbourS) was employed for the validation. NOWPHAS has GPS wave gauges as shown in Figure 3(e). The observation point of Off_Yamagata (Japanese official name: “山形県沖”, 139°36'02"E, 38°58'29"N), was selected in this study. This location is inside of the Sea of Japan, a semi-closed ocean bounded by land and the many islands of Japan. In this area, waves are affected by the islands and limited wind fetches, making it suitable to verify the accuracy of the wave data from the global domain with the observed wave data in specific areas. Hourly wave data collected from the NOAA source at the corresponding time as the observational period were used to compare with those from the NOWPHAS wave database.

The comparison results are shown in the Figure 3. In the period for which observational data are available, the waves computed by WW3 are the same as the observed waves by NOWPHAS in wave height, direction and period. Wave data could not recorded from March 11st - May 31st due to the influence of the Tohoku Earthquake-Tsunami on March 11st. Because the reanalysis wave data provided by WW3_NOAA is highly accurate compared with the actual waves observed by wave gauges. Therefore, the data can be reliably used to assess offshore wave characteristics or boundary conditions for other nearshore wave models.

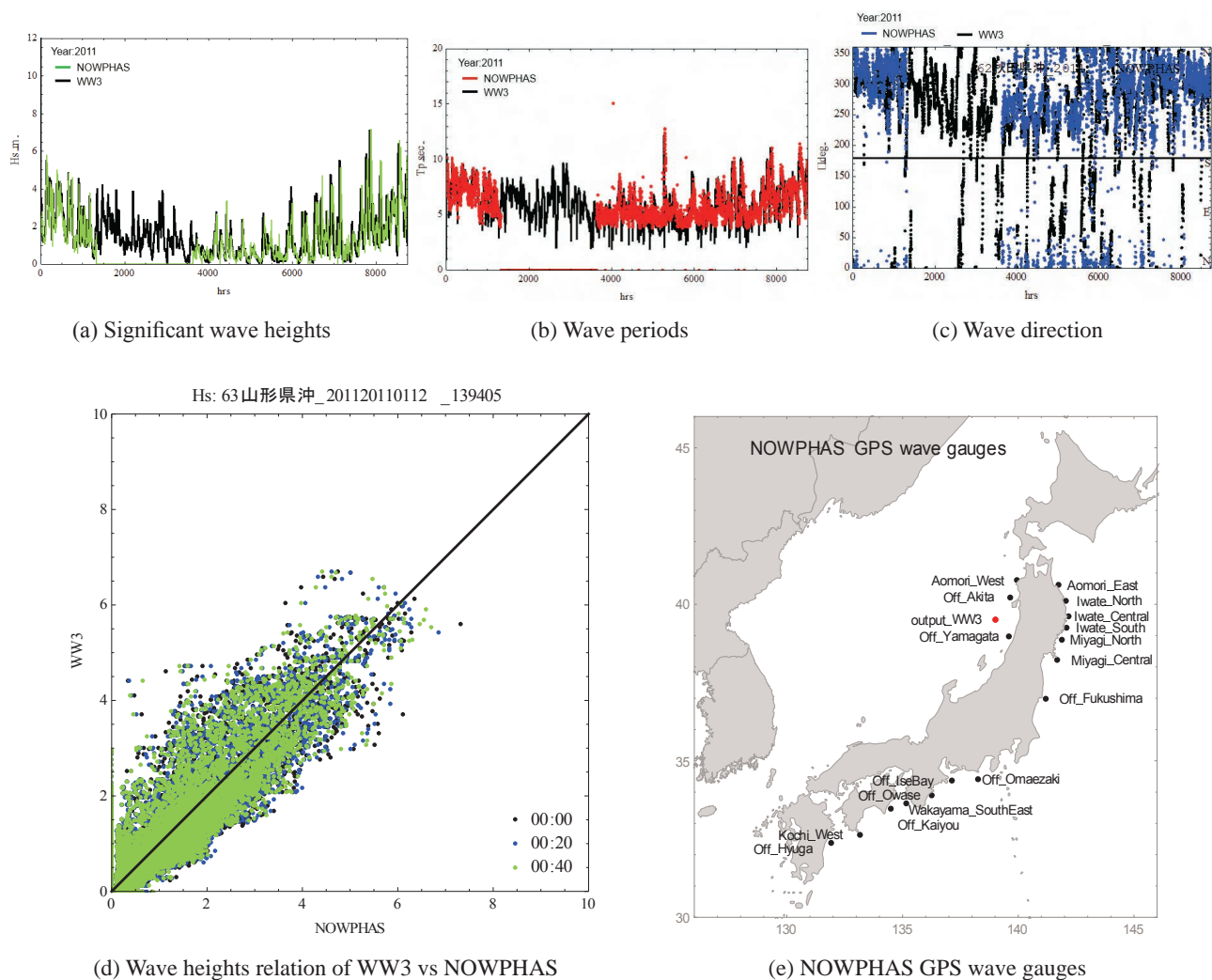


Figure 3. Comparison of reanalysis data by WW3_NOAA and offshore wave observation by NOWPHAS at the point of Off_Yamagata in 2011. GPS observation and WW3 output points are shown in Japanese in (e).

2.3 Offshore wave characteristics in South China Sea

NOAA provides global wave data but these data only available at 1 degree resolution. There are 14 points closest to the coastline having available offshore wave provided by NOAA wave database (see Figure 4). Because the Vietnamese coastal zone is divided into 4 regions: north (P1-P3 in Figure 4), north-central (P4-P6), south-central (P7-P10) and south (P11-P14) regions,

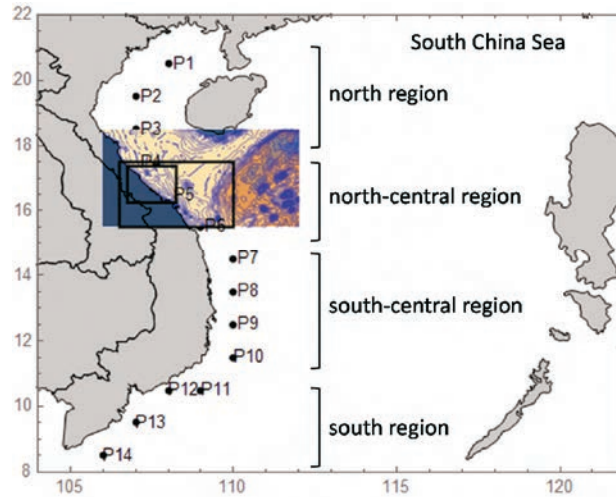


Figure 4. Offshore WW3 wave points along the Vietnam coast (P1-P14) and Computational domain (Domain-1 and Domain-2)

choosing one point in each region to display wave characteristics of the region. The seasonal changes in offshore wave parameters along the Vietnamese coast of 9 years from 2005 to 2013 are summarized below.

(a) North Region (P1-P3)

Seasonal changes in offshore wave parameters at P3 of Figure 4 are shown in Figure 5.

- Highest wave (Hs: 8m) appeared in September and October with long wave periods (Tp:10-15s) which may be generated by typhoon.
- In winter large wave height ranges 3 to 5m. Its wave period is 10-12s.
- Low wave season is June to August with wave direction SW-SE. Average wave height is less than 1 m. Even in low wave season, several spontaneous high waves (Hs:3-4m) are generated.

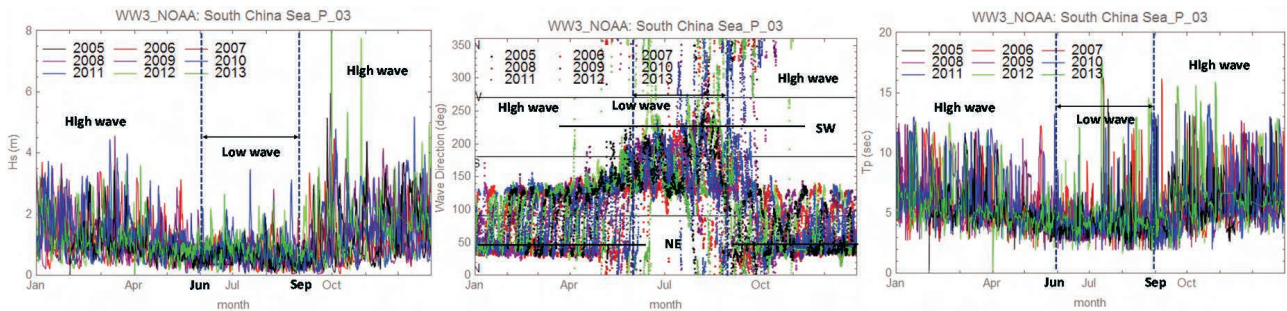


Figure 5. Seasonal changes in offshore wave parameters in North region (2005-2013)

(b) North-Central Region (P4-P6)

Seasonal changes in offshore wave parameters at P5 of Figure 4 are shown in Figure 6.

- Similar to North region, the highest wave (Hs: 7m) appears in September and October with long wave periods (Tp:10-15s) which may be generated by typhoon.
- Winter wave height is a little lower than North region of which significant height is lower than 4m. Winter wave period is also shorter, 8-10s.
- Low wave season is June to August with wave direction SE-E and wave height is less than 1m. Similar to North region, several spontaneous high waves (Hs:2-3m) are generated.

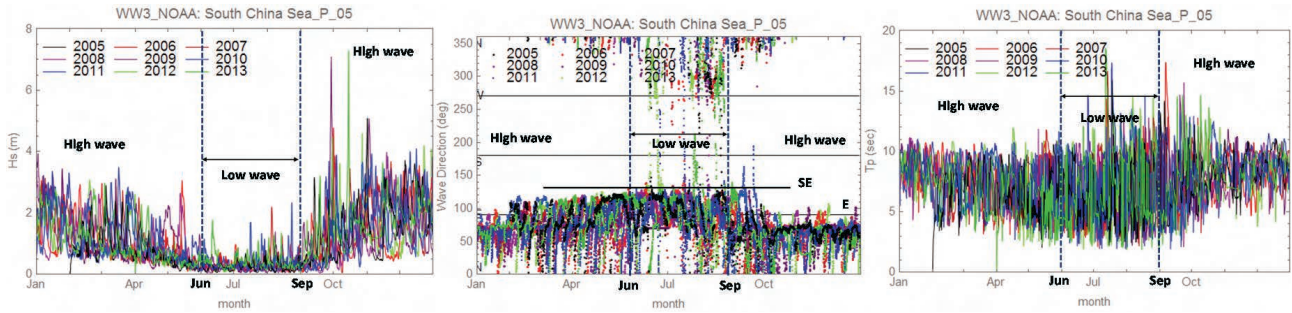


Figure 6. Seasonal changes in offshore wave parameters in North-central region (Hue province) (2005-2013)

(c) South-Central Region (P7-P10)

Seasonal changes in offshore wave parameters at P9 of Figure 4 are shown in Figure 7.

- Wave energy in this region is strongest.
- High waves (Hs: 5-6m) appear in November to next year March with wave periods (Tp:5-10s) which may be generated by winter monsoon with wave direction NE.
- April to September is a low wave season with wave direction SSW. Its wave height ranges 1m to 3m and wave period 3s to 7s.

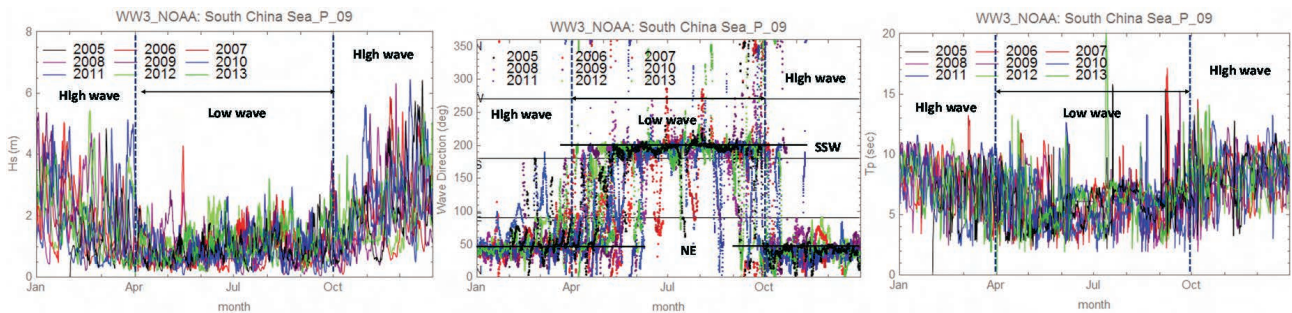


Figure 7. Seasonal changes in offshore wave parameters in South-central region (2005-2013)

(d) South Region (P11-P14)

Seasonal changes in offshore wave parameters at P13 of Figure 4 are shown in Figure 8.

- Wave energy in this region is lowest.
- High waves (Hs: 2-3m) appear in October to next year April with wave periods (Tp:5-10s) which may be generated by winter monsoon with wave direction ENE.
- May to September is a low wave season with major wave direction SW and wave period around 4s.

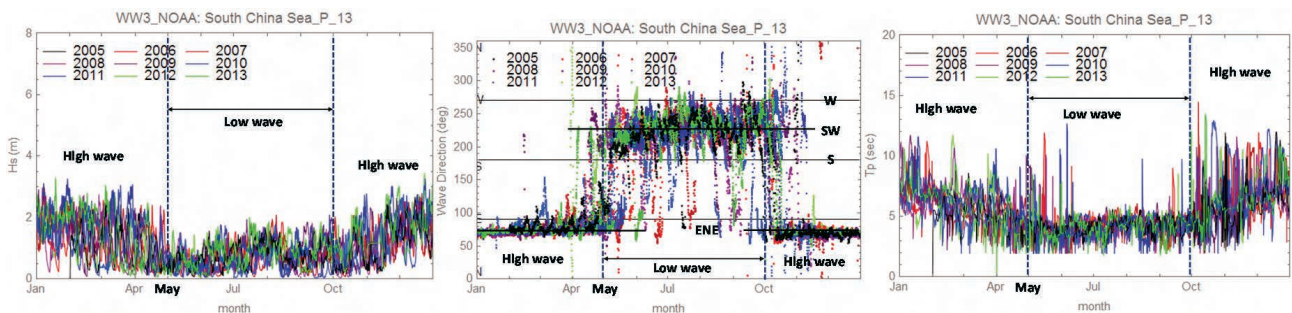


Figure 8. Seasonal changes in offshore wave parameters in South region (2005-2013)

3. Coastal Wave Reanalysis by SWAN Model

3.1 SWAN model

SWAN (Booij et al., 1999⁵) was the first third-generation spectral wave model explicitly designed for nearshore applications. In addition to the processes of wind input, nonlinear four-wave interactions, white-capping and bottom friction dissipation typically accounted for in basin-scale wave models, the nearshore processes of depth-induced breaking and nonlinear three-wave interactions were also incorporated. This allowed practical application to coastal regions using time steps that are appropriate to the time scales of the physical phenomena modeled, as opposed to scales imposed by the numerical framework.

Differing from deep-water wave models, SWAN contains the appropriate physics to simulate processes occurring in shallow waters. It is a third-generation wave-action model developed to simulate wave parameters in coastal areas. This model uses typical formulations for wave growth due to wind, wave dissipation due to white-capping and non-linear wave-wave interactions. In addition, it includes physical processes associated with intermediate depths and shallow water, such as bottom friction and depth-induced wave breaking. The governing equation of the SWAN model is the spectral action balance equation. The change in wave energy density $E(\sigma, \theta)$ depends on the processes of wind-wave generation and growth (S_{in}), wave development (S_{nl}), and wave decay (S_{in} , S_{ds} , S_{bot}):

$$\frac{\partial}{\partial t} N + \frac{\partial}{\partial f} C_f N + \frac{\partial}{\partial \theta} C_\theta N + \frac{\partial}{\partial x} C_x N + \frac{\partial}{\partial y} C_y N = \frac{1}{\sigma} (S_{in} + S_{nl} + S_{ds,w} + S_{ds,br} + S_{bot}) \quad (1)$$

in which:

- S_{in} : the transfer of energy from wind to waves
- S_{nl} : the dissipation of wave energy due to nonlinear wave-wave interactions
- $S_{ds,w}$: the dissipation of wave energy due to white-capping
- $S_{ds,br}$: the dissipation of wave energy due to depth-induced breaking
- S_{bot} : the dissipation of wave energy due to bottom friction
- N : wave action density spectrum that is equal to the energy density divided by the relative frequency, ($N(x,y,\sigma,\theta)=E(\sigma,\theta)/\sigma$),
- σ : the relative frequency considering the current effects, f : the wave frequency
- θ : the wave direction
- C : the propagation velocity of wave action in (x, y, f, θ) space

$\frac{\partial}{\partial x} C_x N$, $\frac{\partial}{\partial y} C_y N$: the propagation of wave action in geographical space

$\frac{\partial}{\partial f} C_f N$: the shifting of the relative radian frequency f due to variations in mean current and depth.

$\frac{\partial}{\partial \theta} C_\theta N$: depth- and current-induced refraction

The left-hand side is the kinematic portion of the above equation and the right hand-side contains the source/sink term that represents all physical processes, including generation, dissipation, and redistribution of wave energy. The component S_{in} represents the energy transfer from wind to ocean waves. The energy input by this mechanism contributes to the initial stages of wave growth. When the sea surface moves up and down, the pressure also follows the same movements, thereby transferring energy to the wave and causing it to grow. The component S_{nl} represents wave energy spectrum change due to nonlinear wave-wave interactions. The physical meaning of the interactions is the exchange of energy between the resonant sets of the wave components, redistributing energy over the spectrum. In deep water, quadruplet wave-wave interactions dominate the evolution of the spectrum. They transfer wave energy from the spectral peak to lower frequencies (thus moving the peak frequency to lower values) and to higher frequencies where the energy is dissipated by white-capping. In very shallow water, triad wave-wave interactions transfer energy from lower frequencies to higher frequencies, resulting in higher harmonics.

The $S_{ds,w}$ part shows the dissipation of wave energy due to white-capping. White capping is primarily controlled by the steepness of waves. The component $S_{ds,br}$ displays the dissipation of wave energy due to depth-induced breaking. When waves propagate towards the shore, shoaling leads to an increase in wave height. When the ratio of wave height over the water depth exceeds a certain limit, waves begin to break, thereby dissipating energy rapidly. In extreme shallow water (surf zone), this process becomes dominant over all other processes. The last component S_{bot} indicates the dissipation of wave energy due to bottom friction.

In this study, wave energy dissipations due to white-capping and depth-induced breaking are saved as a SWAN output dataset. The former wave energy dissipation represents a wave shear stress on the sea surface, and the latter is the driving force of nearshore currents inside the surf zone.

3.2. Model setup for SWAN computation

All quantities that are used in SWAN model are expressed in S.I. units: m, s and composites of these with accepted compounds such as Newton (N) and Watt (W). Consequently, the wave height and water depth are in meter (m), wave period in second (s), etc. Wind and wave directions are used in nautical convention, in degree. The nautical convention means the direction where the wind or the waves come from, measured clockwise from geographic North.

Moreover, due to the hypothesis of SWAN, at the boundary position of the computational domain, only waves from inside the domain can propagate outside, and waves from outside cannot enter the computational area. Therefore, there are errors at the boundary. These errors can be abandoned if the boundary condition is taken from a previous run that has a computational domain overlapping the current computational domain. Thus, this research runs SWAN for 2 nesting domains, a coarse run for larger computational domain (from 106.5° E to 110° E in longitude and from 15.5° N to 17.5° N in latitude) to get wave boundary condition for a smaller domain (from 107.75° E to 108.25° E in longitude and from 16.25° N to 17.375° N in latitude) as in the Figure 4.

With the purpose of calculating wave condition continuously in specific period, non-stationary mode is chosen to run SWAN model. This mode has huge advantage such as reflecting the real condition of input data such as wind, wave boundary and output data wave condition continuously in computational period, however the mode takes a lot of time to finish wave simulation. Furthermore, as in the above analysis, offshore waves change seasonally. Therefore, choose one year in the period 2005-2013 which available offshore wave data to calculate wave regime in Hue nearshore area.

Over these years, offshore waves were essentially divided into 2 seasons, the summer season from April to September and the winter season from October to March of the following year. The wave height in winter is much larger than in summer, especially under the impact of storms and tropical depressions. Regarding offshore wind, the dominant direction is east-southeast. In addition, the year 2006 displays all of the common characteristics of offshore wind and waves in 2005-2013, and some observed wave data was obtained for some periods in 2006. Hence, 2006 was chosen as the computational year in this thesis. The offshore wave parameters provided by WW3_NOAA in 2006 are shown in Figure 9, which are the boundary conditions for SWAN computation.

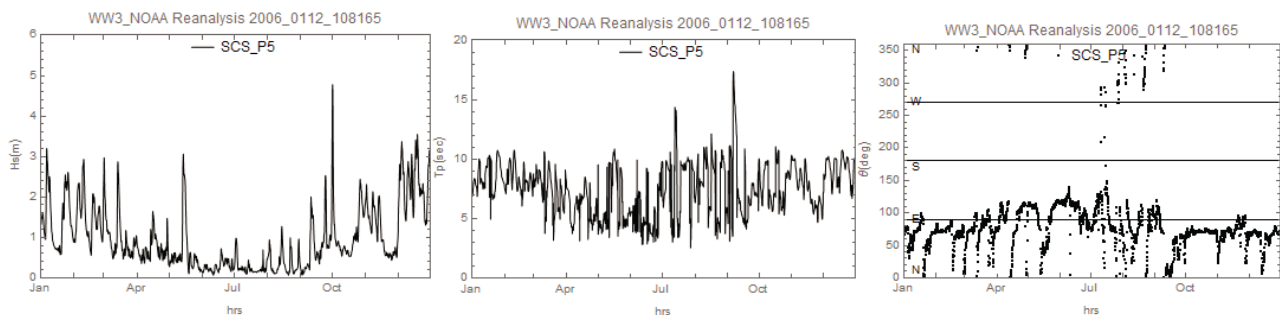


Figure 9. Offshore wave parameters provided by WW3_NOAA in 2006 for the boundary conditions of SWAN computation

3.3. Data used for computation

(a) Bathymetry data

The bathymetry is provided by the GEneral Bathymetric Chart of the Oceans (GEBCO) with an original spatial resolution of 30 arc-seconds. Then it is interpolated into 10 arc-seconds for nested bathymetry. Bathymetries are prepared for 2 runs: coarse run (from 106.5° E to 110° E in longitude and from 15.5° N to 17.5° N in latitude) and nested run (from 107.75° E to 108.25° E in longitude and from 16.25° N to 17.375° N in latitude). In coarse run, bathymetry is displayed in nautical convention longitude and latitude and in nested run, it is displayed through number of element of rectangular mesh, in which the mesh size is 0.0027 degree. Figure 4 shows the topography of the computational domains (domain-1 and domain-2) and offshore wave output points along the coast.

(b) Wind input data

Wind input data are supplied by the National Centers for Environmental Prediction, Final Global Analysis (NCEP FNL) with a spatial resolution of 1 degree. They are the time-series data, downloaded for the computational year 2006. Then, the wind data are interpolated into a spatial resolution of 0.0083 degree in coarse run and 0.0027 degree in nested run. An example of wind input is displayed in Figure 10.

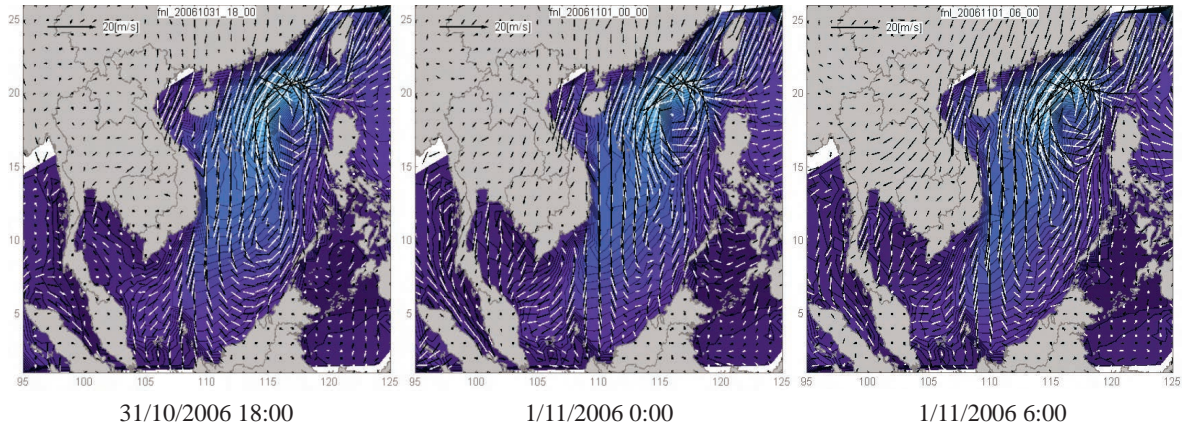


Figure 10. An example of wind vector fields used for SWAN simulation, and the density plot of WW3 significant wave heights, H_s , in the South China Sea (0 - 6m legend bar).

(c) Wave boundary condition with SEGMENT

SWAN command “BOUNDSPEC” defines parametric spectra at the boundary. It consists of two parts, the first part defines the boundary SIDE or SEGMENT where the spectra will be given, the second part defines the spectral parameters of these spectra (see Appendix).

4. Simulation results

The output results of SWAN model include: significant wave height (in m), mean wave direction (in degree, nautical convention), mean absolute wave period (in s), total energy dissipation (in W/m^2), energy dissipation due to surf breaking (in W/m^S), energy dissipation due to white-capping (in W/m^S). They are visualized for whole Hue coastal area.

4.1 A comparison of SWAN outputs and observation in October 2006

Before using SWAN to calculate waves from the offshore ocean propagating to the nearshore area, it is necessary to validate the model. However, due to the limited observed wave data in the research area, only observed waves from a short period in 2006 near Con Co island were collected. Moreover, because the quality of this observed data was not good enough to validate the model, the waves computed by SWAN were only compared with the observed waves from September 28th, 2006 to October 10th, 2006. The observed data were collected at 17.10°N, 107.21°E; and the computed wave data were extracted from the SWAN model at the same time and position. The comparison results are shown in Figure 11.

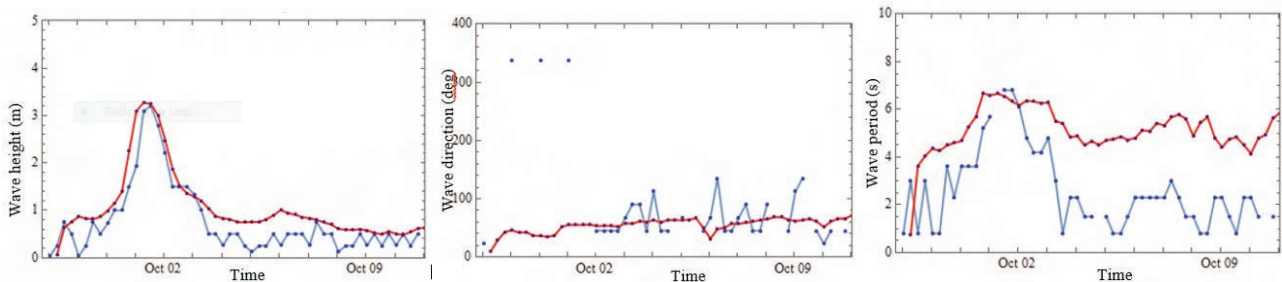


Figure 11. Comparison between computed (red lines) and observed (blue lines) wave parameters of significant wave height, H_s (left), mean wave direction (middle) and peak wave period, T_p (right).

Regarding wave height, the computed and observed peaks are similar, under the impact of storms from September 28th to October 3rd. However, under normal conditions from October 4th to October 10th, the computed and observed wave heights are different, with an average observed wave height of approximately 0.5 m and an average computed wave height of approximately 0.65 m.

In terms of wave direction, the main direction of waves in chosen period is east-northeast. In addition, the output of the SWAN model shows that the main wave direction is also east-northeast. In the observed data, waves also had a north-northwest

direction that appears three times in the observation period. This can be explained by the influence of turbulence in the storm.

The other wave parameter is the period. In special conditions (storm conditions from September 30th to October 3rd), the average observed period is 4.95 s, and, in normal conditions from September 28th to September 29th and from October 4th to October 10th, the average observed period is 1.75 s. From the SWAN model output, the computed wave period is 5.91 s in special conditions and 5 s in normal conditions. Therefore, the computed wave period is different than observed one.

From the above comparison, wave heights and periods are acceptable between computed and observed data. The low technology used in the 2006 wave observations and the lack of detailed bathymetry measurements in the area around the Hue coastline are considered the main causes of differences between computed and observed data.

4.2 Output of reanalysis database in Hue coast

After analyzing the wave climate in 2006, the nearshore wave climate in Hue coast has been saved as output files which can be used for the re-analyzed wave parameters at every hour interval at any output points. An example of SWAN output statements is shown below.

```
BLOCK 'COMPGRID' NOHEAD 'out/JUN.nesD' LAY 4 DIR 1 OUT 20060601.000000 1 HR
BLOCK 'COMPGRID' NOHEAD 'out/JUN.nesH' LAY 4 HS 1 OUT 20060601.000000 1 HR
BLOCK 'COMPGRID' NOHEAD 'out/JUN.nesT' LAY 4 PER 1 OUT 20060601.000000 1 HR
BLOCK 'COMPGRID' NOHEAD 'out/JUN.nesW' LAY 4 WIND 1 OUT 20060601.000000 1 HR
BLOCK 'COMPGRID' NOHEAD 'out/JUN.nesDSP' LAY 4 DISSIP 1 OUT 20060601.000000 1 HR
BLOCK 'COMPGRID' NOHEAD 'out/JUN.nesDSPSRF' LAY 4 DISSURF 1 OUT 20060601.000000 1 HR
BLOCK 'COMPGRID' NOHEAD 'out/JUN.nesDSPWCP' LAY 4 DISWCAP 1 OUT 20060601.000000 1 HR
```

In this statement, DIR is wave direction, HS: significant wave height, PER: peak wave period, WIND: wind vector (x, y), DISSP: total energy dissipation, DISSURF: wave energy dissipation due to depth-induced breaking, DISWCAP: wave energy dissipations due to white-capping. (TUDELFT. SWAN^(6,7,8,9))

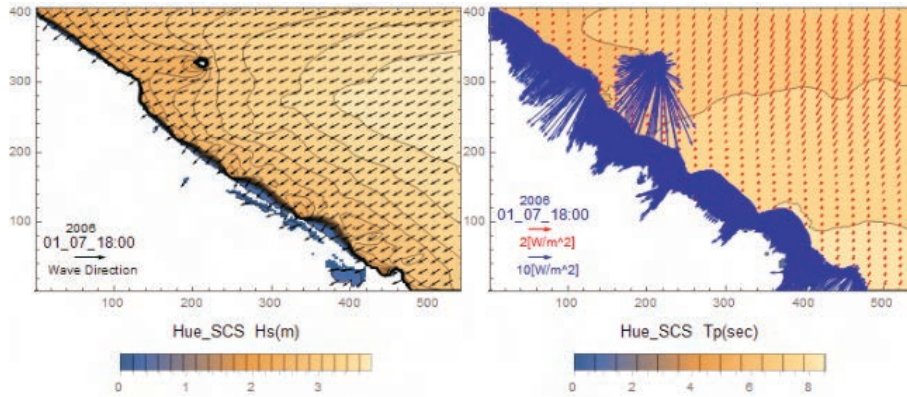
The typical winter wave output of DIR, HS, PER, DISSURF and DISWCAP are shown in Figure 12, in which left figure indicates wave height and direction, right figure indicates wave energy dissipation and wave periods. Blue arrows in the surf zone shows the wave energy dissipation rate due to depth-limited breaking that extends to 100 W/m², and red arrows show wave energy dissipation rate due to white capping in the offshore of which order is 1-2 W/m⁵. These energy dissipation rates provide the external forces of current generation through the mechanism energy mode changes from wave to currents. This energy transfer can be computed by following equation.

$$\tau_{break} = \rho g \iint \frac{S_{ds}(f, \theta)}{C(f)} df d\theta \quad (2)$$

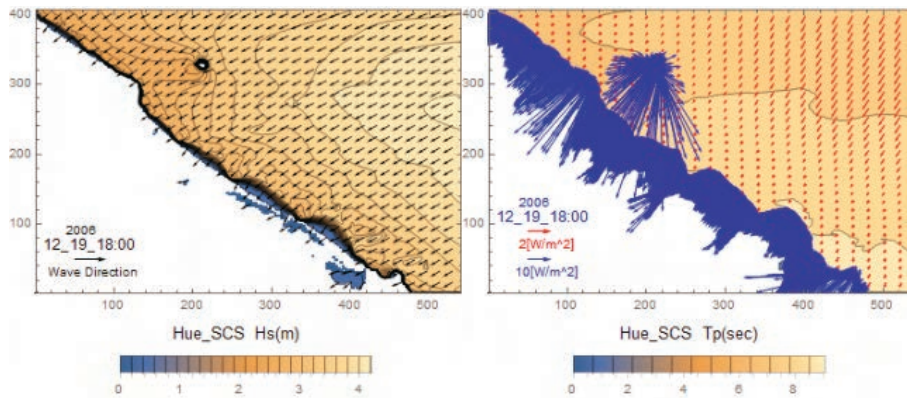
where, τ_{break} is the shear stress on the sea surface caused by energy transfer from wave to current, $S_{ds}(f, \theta)$ the wave energy dissipation rate, ρ the sea water density, and g the gravitational acceleration.

From the reanalysis database, seasonal changes in wave characteristics in Hue coast can be summarized below.

- Summer wave climate from April to September: the wave direction is mainly from south to north, with detailed directions such as south-west and south-east. The wave height is quite small. Due to the small wave height, waves have little energy, resulting in little wave energy dissipation due to surf-breaking and white-capping. Within the shallow area, the wave direction is nearly parallel with the shoreline. However, the wave height is very small.
- Winter wave climate from October to March: the wave direction is mainly from north to south, with detailed directions such as north-east and east. The wave height in the winter season is much larger than in the summer. The wave energy in the winter period is greater than in the summer; therefore, wave energy dissipation due to surf-breaking and white-capping is also greater than those in summer. Within the shallow area, the wave direction is mostly perpendicular to the coastline.



(a) January 7th 18:00



(b) December 19th 18:00

Figure 12. The typical winter wave output of DIR(Wave Direction), HS(Hs), PER(Tp), DISSURF (blue arrows) and DISWCAP(red arrows). (from the established database of Hue coastal waves)

4.3 Coastal wave parameters and wave energy along 20m depth contour

Coastal wave output along the 20 m depth contour depicts the characteristics of incoming waves because of the just before depth-limited breaking. It may be able to use for design solutions to protect beaches. Figure 13 shows the selected points along 20m depth contour line to save the wave data computed. Points numbered 10 to 26 are inside the Hue province domain.

Regarding the directional characteristics of incoming wave energy flux, directional distribution of the wave period (smaller than 3.5s are neglected) and wave height are necessary information (left of Figure 16). The directional wave energy flux intensity (annual average of $H_s^2 \cdot T_p$) are shown in right of Figure 14 for output points P10, P18 and P26. A long green line indicates the coastline of Hue province and the short one is its normal direction. The wave characteristics can be clearly divided into two seasons, a summer wave climate from April to September and a winter wave climate from October to March. The left side figures are winter high wave condition and the right are summer low wave condition.

From Figure 14, the directional distribution of wave parameters and wave energy flux intensity are summarized as follows:

- A dominant wave incident is a little right side from the shore normal in both winter and summer.
- In summer, wave window (a possibility of the incident wave direction) is very narrow, and the wave heights are quite small with an average of approximately 0.5 m. Due to the very small wave height, the wave energy flux was also inappreciable in summer.

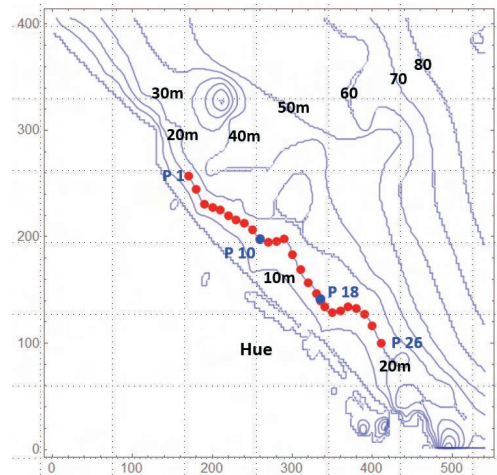


Figure 13. Output points on the 20m depth contour along the Hue coast (P1-P26).

- In winter, the dominant wave direction is NE. The wave height in winter was much higher than in summer, with an average of about 1.7 m. Therefore, the wave energy in the winter season was much greater than in summer.
- Total coastal wave energy flux has a power of NW wards current generation that transport sediment from SE to NW inside the surf zone at any points along the Hue coast.

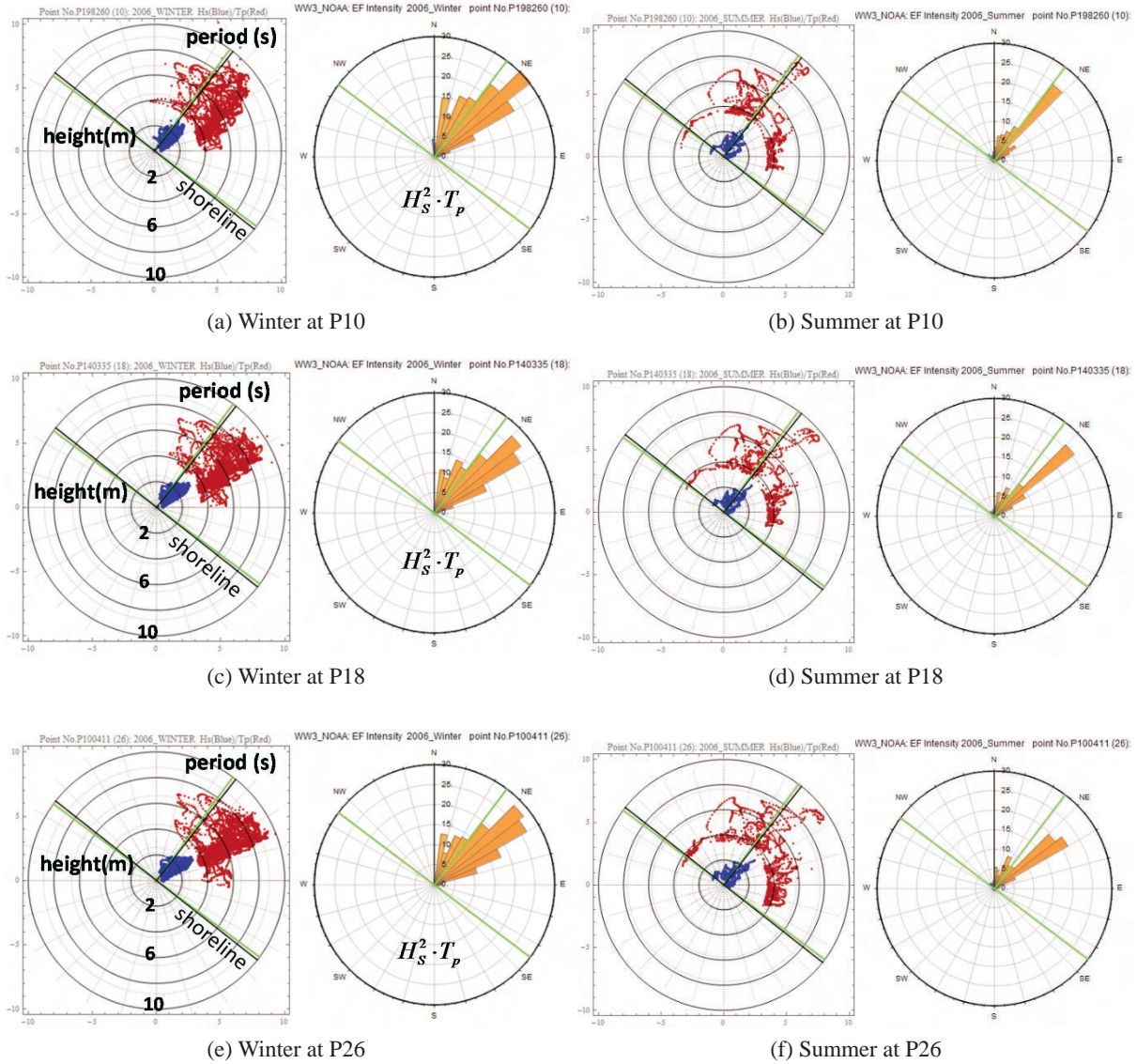
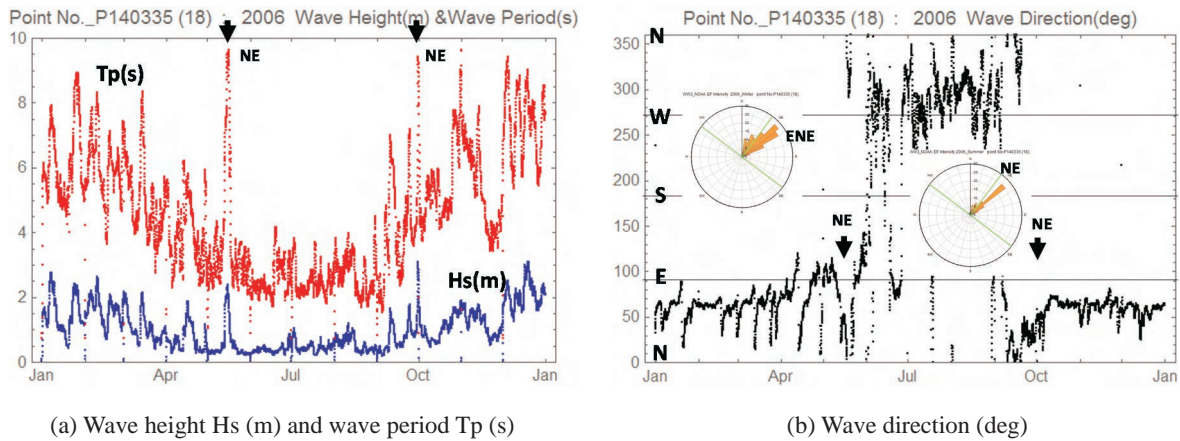


Figure 14. Directional distribution of wave parameters H_s (blue) and T_p (red) in the left figure. Annual average of wave energy flux intensity, $H_s^2 \cdot T_p$ in the right figure at the points of P10, P18 and P26 in Figure 13.

Figure 15 shows annual changes in wave height and wave period (a) and wave direction (b) at the output point, P18 in Figure 13, just offshore of Hue inlet. In summer, the computed wave direction shows NW-W that is wave from the land. This offshore-going waves may be generated by wind blowing from land to offshore in summer which generates a small wave from the shore to 20m-depth position. These wave heights are less than 0.5m and periods shorter than 3.5s that are neglected wave components in Figure 14. The highest wave in winter is 3m in height and 9.5s in period. Two cases of long period and high wave are computed in the middle of May and the beginning of October in Figure 15 which were caused by typhoon. The dominant breaking wave direction in the nearshore are E-NE-N, in both winter monsoon and summer typhoon resulting in the dominant NW longshore currents in Hue coast.

(a) Wave height H_s (m) and wave period T_p (s)

(b) Wave direction (deg)

Figure 15. Annual changes in the wave parameters computed by SWAN in 2006 at the point P18 (20m deep)

5. Conclusions

A wave characteristics along the Vietnam coasts facing the South China Sea in which well-organized wave observations have not been developed, were made clear in this study using the ocean wave reanalysis data provided by WW3_NOAA that is global analysis program by the third generation ocean wave model, WW3.

Hourly changes in the significant wave height, wave period and wave direction in the offshore waves in the northern, north-central, south-central central, and southern coasts have been analyzed since February, 2005 up to December 2014. Then to analyze the wave characteristics in the coastal zone, wave deformation computation by shallow water wave model SWAN was carried in 2006 at the north-central Vietnam coast of Hue. As wave boundary conditions in this case, significant wave height, the peak period and peak wave direction of WW3_NOAA were imposed by using the SEGMENT boundary method.

The main results obtained in this study are listed below.

- (1) Validation of offshore wave database of WW3_NOAA: The accuracy of WW3_NOAA reanalysis data was checked by comparing with Japan's reliable wave observation system NOWPHAS (Nationwide Ocean Wave information network for Ports and HarbourS) GPS wave gauge inside of the Sea of Japan, a semi-closed ocean bounded similar to the South China Sea. It was confirmed that WW3_NOAA data can be reliably to use as an offshore boundary condition for the coastal wave simulation.
- (2) Offshore wave characteristics in South China Sea was made clear with WW3_NOAA reanalysis data obtaining the following results.

North Region:

- In winter large wave height ranges 3 to 5m. Its wave period is 10-12s.
- Low wave season is June to August with wave direction SW-SE. Average wave height is less than 1m. Even in low wave season, several spontaneous high waves (H_s :3-4m) are generated.

North-Central Region:

- Similar to North region, the highest wave (H_s : 7m) appears in September and October with long wave periods (T_p :10-15s) which may be generated by typhoon.
- Winter wave height is a little lower than North region of which significant height is lower than 4m. Winter wave period is also shorter, 8-10s.

South-Central Region:

- Wave energy in this region is strongest. High waves (H_s : 5-6m) appear in November to next year March with wave periods (T_p :5-10s) which may be generated by winter monsoon with wave direction NE.
- April to September is a low wave season with wave direction SSW. Its wave height ranges 1m to 3m and wave period 3s to 7s.

South Region:

- Wave energy in this region is lowest. High waves (H_s : 2-3m) appear in October to next year April with wave periods (T_p :5-10s) which may be generated by winter monsoon with wave direction ENE.
- May to September is a low wave season with major wave direction SW and wave period around 4s.

- (3) SWAN simulation model was briefly validated with the shallow wave observation data at Hue coast in October, 2006.
- (4) Coastal reanalysis dataset was established by SWAN simulation in Hue coastal zone in 2006. The nearshore wave parameters at every hour interval at any output points in Hue coast can be reproduced by this dataset.
- (5) The directional distribution of wave parameters and wave energy flux intensity are also made clear as below.
 - A dominant wave incident is a little right side from the shore normal in both winter and summer.
 - In winter, the dominant wave direction is NE. The wave height in winter was much higher than in summer, with an average of about 1.7 m. Therefore, the wave energy in the winter season was much greater than in summer.
 - Total coastal wave energy flux has a power of NW wards current generation that transport sediment from SE to NW inside the surf zone at any points along the Hue coast.
- (6) Considering the wave energy transfer mechanism to the nearshore currents. The dominant direction of coastal currents in Hue coast was estimated to be NW.

REFERENCES

1. Tran.T. T, Nguyen. D. D, 2013. Study on hydrodynamics conditions, sediment transport and evaluation of beach nourishment for Cua Tung beach, Quang Tri. Hydrological and environment science, pp.21-29.
2. WAMDIG, 1988: The WAM model-a third generation ocean wave prediction model. J. Phys.Oceanogr., 18, pp.1775-1809.
3. Tolman, H. L., 1991: A third-generation model for wind waves on slowly varying, unsteady and inhomogeneous depths and currents. J. Phys. Oceanogr., 21, pp.782-797.
4. Jeffrey L. Hanson, Barbara A. Tracy, Hendrik L. Tolman, and R. Douglas Scott, 2009: Pacific Hindcast Performance of Three Numerical Wave Models. J. Atmos. Oceanic Technol., 26, pp.1614-1633.
5. Booi, N., R. C. Ris and L. H. Holthuisen, 1999: A third-generation wave model for coastal regions, Part I, Model description and validation. J. Geophys. Res., 104, pp.7649-7666.
6. TUDELFT. *SWAN - Implementation manual*. Delft University of Technology, Environmental Fluid Mechanics Section, <http://www.swan.tudelft.nl>
7. TUDELFT. *SWAN - Programming rules*. Delft University of Technology, Environmental Fluid Mechanics Section, <http://www.swan.tudelft.nl>
8. TUDELFT. *SWAN - Scientific and Technical documentation*. Delft University of Technology, Environmental Fluid Mechanics Section, <http://www.swan.tudelft.nl>
9. TUDELFT. *SWAN - User manual*. Delft University of Technology, Environmental Fluid Mechanics Section, <http://www.swan.tudelft.nl>

APPENDIX

SWAN command “BOUNDSPEC” defines parametric spectra at the boundary as shown in Figure A-1.

```

BOUNdspec <
| North |
| NW |
| West |
| SW | | -> CCW |
| -> SIDE < South > < |
| | | | CLOCKwise | |
| | | East | |
| | | NE | |
BOUNdspec < > &
| -> XY < [x] [y] > |
| SEGment < > |
| IJ < [i] [j] > |
|
| PAR [hs] [per] [dir] [dd] |
| CONstant < |
| FILE 'fname' [seq] |
|
|
| PAR < [len] [hs] [per] [dir] [dd] > |
| VARiable < |
| FILE < [len] 'fname' [seq] > |

```

Figure A-1. Format of SWAN command “BOUNDSPEC”

SEGMENT is used if SIDE is not used, i.e. either the boundary segment goes around a corner of the grid, or the segment is only part of one side of the grid. The distance along the segment is measured from the first point of the segment with command of XY. The segment is defined by means of a series of points in terms of problem coordinates; these points do not have to coincide with grid points. The (straight) line connecting two points must be close to grid lines of the computational grid (the maximum distance is one hundredth of the length of the straight line).

FILE means that the incoming wave data are read from a file. There are three types of FILE:

- TPAR files containing non-stationary wave parameters,
- files containing stationary or non-stationary 1D spectra (usually from measurements),
- files containing stationary or non-stationary 2D spectra (from other computer programs or other SWAN runs).

A TPAR file is for only one location; it has the string TPAR on the first line of the file and a number of lines which each contain 5 numbers, i.e.:

Time (ISO-notation), Hs, Period (average or peak period depending on the choice given in command BOUND SHAPE), Peak Direction (Nautical or Cartesian, depending on command SET), Directional spread (in degrees or as power of cos depending on the choice given in command BOUND SHAPE).

Example of a TPAR file:

```
TPAR
19920516.1300 4.2 12. -110. 22.
19920516.1800 4.2 12. -110. 22.
19920517.0000 1.2 8. -110. 22.
```

Wave boundary for coarse run in this study are identified by continuously segments as in the Figure A-2. There are 9 segments from S1 to S9 that create continuous open-boundary of the coarse run. Each segment has one point available offshore wave parameters from WW3_NOAA database: P1(107°E, 17.5°N); P2(108°E, 17.5°N); P3(109°E, 17.5°N); P4(110°E, 17.5°N); P5(110°E, 16.5°N); P6(110°E, 15.5°N); P7 (109°E, 15.5°N). For “SEGMENT XY” type boundary condition, the statements of the SWAN input file is shown in the right-hand side of Figure 12. Wave boundary condition for nesting computation is extracted from output from the coarse run.



Figure A-2. Wave boundary condition by SEGMENT method